Hindawi
Mathematical Problems in Engineering
Volume 2019, Article ID 2547891, 14 pages
https://doi.org/10.1155/2019/2547891

Research Article

Research on Multiple Griffith Cracks at the Interface of Fine-Grained Piezoelectric Coating/Substrate

Shuaishuai Hu,[1] **Jiansheng Liu**,[1] **and Junlin Li**[2]

[1]*School of Materials Science and Engineering, Taiyuan University of Science and Technology, Taiyuan 030024, China*
[2]*School of Applied Science, Taiyuan University of Science and Technology, Taiyuan 030024, China*

Correspondence should be addressed to Junlin Li; lijunlin9762@163.com

Received 3 May 2019; Accepted 30 July 2019; Published 19 August 2019

Academic Editor: Francisco J. Montáns

The behavior of a fine-grained piezoelectric coating/substrate with multiple Griffith interface cracks under electromechanical loads is investigated. In this work, double coupled singular integral equations are proposed to solve the fracture problems. Both the singular integral equation and single-valued conditions are simplified into an algebraic equation and solved by numerical calculation. Thereby, the intensity factors of electric displacement and stress obtained are used to obtain the expression of the energy release rate. Furthermore, numerical results of the energy release rate with material parameters are demonstrated. Based on the obtained results, it could be concluded that the energy release rate is closely related to the size of the interface cracks and the mechanical-electrical loading. For a bimaterial structure, the fine-grained piezoelectric structure exhibited better material performance compared to the large one.

1. Introduction

Piezoelectric bimaterials have been widely applied in many fields, such as sensors, actuators, filters, and storage devices. Owing to the reliability of composite materials, double-layer bonded bimaterial composite structures have played an important role in smart structures. However, piezoelectric composites tend to crack, fracture, and debond at the interface during the process of fabricating defects and load conditions [1]. Therefore, the issue of defects of piezoelectric materials under electromechanical load has attracted wide attention [2–7]. Viun et al. [8] handled the interface problems of bi-piezoelectric materials under tensile mechanical loads and electric displacements. The influence of material parameters on finite-sized piezoelectric plates is analyzed by a finite-element method. Li et al. [9] analyzed the mechanical properties of static and dynamic interface cracks of functionally graded coatings/substrates. In this work, the Fourier transform and Laplace transform were used as the fundamental solutions to solve the problem under static and dynamic loads. Soh et al. [10] studied the behavior of bi-piezoelectric ceramic strips with mode III central interface cracks, and the influences of thickness and material coefficients of piezoelectric strips on intensity factors and stress were obtained. Shavlakadze [11] demonstrated the electroelastic contact problem of piezoelectric plates with elastic coatings. By using the method of analytic function theory, the problem was reduced to a singular integrodifferential equation with fixed singularity. Shin and Kim [12] studied the transient response of mode III interface cracks between the piezoelectric layer and the functional orthotropic material layer. The integral equations were solved by the integral method, and it was concluded that the material parameters could prevent the transient fracture of the interface crack. Gherrous and Ferdjani [13] investigated a Griffith interface crack of bi-piezoelectric materials, and the singular integral equations were reduced into algebraic equations by using Chebyshev polynomials. Nan and Wang [14] studied the effect of residual surface stress on the stress and electric field strength of conductive cracks in piezoelectric nanomaterials. The numerical results showed that the residual stress had a significant effect on the piezoelectric nanomaterials, and the piezoelectric nanomaterials had stronger electromechanical coupling compared to the

classical fracture mechanics. Nourazar and Ayatollahi [15] examined the effects of multiple interface cracks in orthotropic-strip-bonded bi-piezoelectric strips, and the results reflected the crack size had a great influence on the intensity factor and the hoop stress of the cavities. Tian and Rajapakse [16] studied a penny-shaped interface crack of double piezoelectric materials, and the Hankel integral transformation method was used to establish a mixed boundary-value problem corresponding to an interface crack. Gao et al. [17] investigated a permeable crack problem in infinite magnetoelectroelastic solids with linear coupling between the elastic and electromagnetic fields, and the results showed in the most general cases that the singularity of the electric-magnetic field was always dependent on that of stress. Kozinov et al. [18] considered a periodic set of limited electrically permeable cracks at the interface of two different piezoelectric semi-infinite spaces and analyzed the influence of electric permeability of cracks on electromechanical fields and the fracture mechanical parameters.

However, the piezoelectric materials with defects studied above are large-grained materials composed of multidomain grains from several microns to tens of microns, and the size could not meet the needs. Reducing the particle size to the submicron level can improve the machinability of the material and the mechanical strength of the device. Kim et al. studied the piezoelectric characteristics of fine-grained piezoelectric materials compared with conventionally prepared large-grained piezoelectric materials under certain conditions [19]. In this latter work, the influence of grain size on density, dielectric constant, phase structure, and piezoelectric properties was investigated [20–23]. However, the mechanical properties of fine-grained piezoelectric materials with defects have not been studied.

Although many researchers have studied the interface fracture problems of piezoelectric bi-materials [1], few studies have been done on the interface fracture of fine-grained piezoelectric coating/substrate smart structures. As an important fracture parameter with which to measure structural safety, the energy release rate plays a crucial role in safety checking of structures. In this paper, a fine-grained piezoelectric coating/substrate mechanical model is established to describe the interaction of multiple Griffith interface cracks. The Fourier integral transformation method is used to transform the problem into a singular integral equation to obtain the energy release rate conveniently. Furthermore, the interaction between the energy release rate and material parameters is investigated. The results of the studies indicate that the appropriate stress and electric displacement loads could prevent the growth of cracks and that a thinner coating thickness is more conducive to the safety of the structure. In addition, fine-grained piezoelectric materials have more safety than large-grained ones.

2. Problem Formulation

As shown in Figure 1, the fine-grained ceramic powder was sprayed uniformly to the surface of the piezoelectric substrate by plasma spraying technology to form a coating. A fine-grain piezoelectric coating/substrate structure was

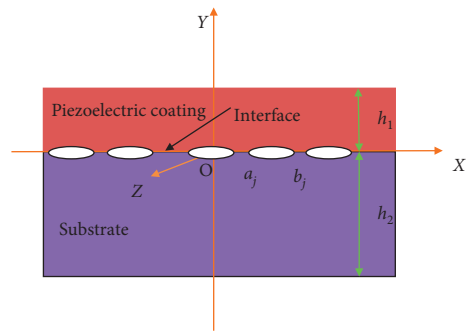

Figure 1: Multiple Griffith interface cracks between the fine-grained piezoelectric coating and the substrate.

obtained by polarization treatment of coating. The thickness of the coating is h_1 and of the substrate is h_2. The rectangular coordinate system was built with the X-axis along the structure interface and the Y-axis along the structure thickness direction. The multiple Griffith interface cracks are 2-dimensional and all within the same orientation and occupying the intervals $x \in (a_j, b_j)$ $(j = 1, 2, \ldots, n)$, respectively. The fine-grained piezoelectric coating and piezoelectric substrate are polarized along the Z-axis, and they are transversely isotropic.

Assume that the problem of the fine-grained piezoelectric coating/substrate interface cracks is considered as only the out-of-plane displacement W and the in-plane electric fields Φ such that

$$\begin{aligned} U &= V = 0, \\ W &= W(x, y), \\ \Phi &= \Phi(x, y). \end{aligned} \tag{1}$$

In this case, the constitutive equations become [4]

$$\sigma_{xz} = c_{44}^{(k)} \frac{\partial W}{\partial x} + e_{15}^{(k)} \frac{\partial \Phi}{\partial x}, \tag{2}$$

$$D_x = e_{15}^{(k)} \frac{\partial W}{\partial x} - \varepsilon_{11}^{(k)} \frac{\partial \Phi}{\partial x}, \tag{3}$$

$$\sigma_{yz} = c_{44}^{(k)} \frac{\partial W}{\partial y} + e_{15}^{(k)} \frac{\partial \Phi}{\partial y}, \tag{4}$$

$$D_y = e_{15}^{(k)} \frac{\partial W}{\partial y} - \varepsilon_{11}^{(k)} \frac{\partial \Phi}{\partial y}, \tag{5}$$

where σ_{xz} and σ_{yz} are the stress components, D_x and D_y are the electric displacement components, $c_{44}^{(k)}$ is the elastic modulus, $e_{15}^{(k)}$ and $\varepsilon_{11}^{(k)}$ are the piezoelectric and dielectric constants, and the superscript k $(k = 1, 2)$ stands for the fine-grained piezoelectric coating and piezoelectric substrate, respectively.

According to Park, the governing equations can be written as follows:

$$c_{44}^{(k)} \nabla^2 W + e_{15}^{(k)} \nabla^2 \Phi = 0, \tag{6}$$

$$e_{15}^{(k)} \nabla^2 W - \varepsilon_{11}^{(k)} \nabla^2 \Phi = 0, \quad k = 1, 2, \tag{7}$$

where ∇^2 is the two-dimensional Laplacian operator.

Assume that there is no loading on the surface of the coating/substrate and the antiplane shear stress σ_0 and in-plane electric displacement D_0 are loaded on the surface of the Griffith interface cracks. Therefore, the mixed boundary conditions of the problems can be written as follows:

$$\sigma_{yz}(x,h_1) = \sigma_{yz}(x,-h_2) = 0, \tag{8}$$

$$D_y(x,h_1) = D_y(x,-h_2) = 0, \tag{9}$$

$$\sigma_{yz}(x,0^+) = \sigma_{yz}(x,0^-), \quad x \notin (a_j,b_j), \tag{10}$$

$$D_y(x,0^+) = D_y(x,0^-), \quad x \notin (a_j,b_j), \tag{11}$$

$$W(x,0^+) = W(x,0^-), \quad x \notin (a_j,b_j), \tag{12}$$

$$\Phi(x,0^+) = \Phi(x,0^-), \quad x \notin (a_j,b_j), \tag{13}$$

$$\sigma_{yz}(x,0^+) = \sigma_{yz}(x,0^-) = -\sigma_0, \quad x \in (a_j,b_j), \tag{14}$$

$$D_y(x,0^+) = D_y(x,0^-) = -D_0, \quad x \in (a_j,b_j). \tag{15}$$

3. Solution to the Problem

By Fourier integral transform of equations (6) and (7), the loading displacement and electric field are obtained, respectively:

$$W(x,y) = \frac{1}{2\pi}\int_{-\infty}^{+\infty}\left[A_{1k}e^{|\alpha|y} + B_{1k}e^{-|\alpha|y}\right]e^{-i\alpha x}d\alpha, \tag{16}$$

$$\Phi(x,y) = \frac{1}{2\pi}\int_{-\infty}^{+\infty}\left[A_{2k}e^{|\alpha|y} + B_{2k}e^{-|\alpha|y}\right]e^{-i\alpha x}d\alpha, \tag{17}$$

where $A_{1k}(\alpha)$, $B_{1k}(\alpha)$, $A_{2k}(\alpha)$, and $B_{2k}(\alpha)$ are the unknown functions $(k = 1,2)$.

Substitution formulas (16) and (17) into equations (4) and (5), the stress and the electric displacement are obtained, respectively:

$$\begin{aligned}\sigma_{yz} = \frac{1}{2\pi}\int_{-\infty}^{+\infty}&\left[c_{44}^{(k)}\left(A_{1k}|\alpha|e^{|\alpha|y} - B_{1k}|\alpha|e^{-|\alpha|y}\right)\right.\\ &\left.+ e_{15}^{(k)}\left(A_{2k}|\alpha|e^{|\alpha|y} - B_{2k}|\alpha|e^{-|\alpha|y}\right)\right]e^{-i\alpha x}d\alpha,\end{aligned} \tag{18}$$

$$\begin{aligned}D_y = \frac{1}{2\pi}\int_{-\infty}^{+\infty}&\left[e_{15}^{(k)}\left(A_{1k}|\alpha|e^{|\alpha|y} - B_{1k}|\alpha|e^{-|\alpha|y}\right)\right.\\ &\left.+ \varepsilon_{11}^{(k)}\left(A_{2k}|\alpha|e^{|\alpha|y} - B_{2k}|\alpha|e^{-|\alpha|y}\right)\right]e^{-i\alpha x}d\alpha.\end{aligned} \tag{19}$$

In order to solve the problem easily, we utilize continuously distributed dislocations to simulate collinear cracks. For this, we introduce the density function as follows:

$$g_W^{(j)}(x) = \frac{d}{dx}\left[W^{(j)}(x,0^+) - W^{(j)}(x,0^-)\right], \tag{20}$$

$$g_\Phi^{(j)}(x) = \frac{d}{dx}\left[\Phi^{(j)}(x,0^+) - \Phi^{(j)}(x,0^-)\right], \quad j = 1,2,\ldots,n. \tag{21}$$

According to equations (12) and (13), the dislocation density function should make the following single-valued conditions valid:

$$\begin{aligned}&\int_{a_j}^{b_j} g_W^{(j)}(t)dt = 0,\\ &\qquad g_W^{(j)}(x) = 0, \quad \text{for } x \notin (a_j,b_j), \quad j = 1,2,\ldots,n,\\ &\int_{a_j}^{b_j} g_\Phi^{(j)}(t)dt = 0,\\ &\qquad g_\Phi^{(j)}(x) = 0, \quad \text{for } x \notin (a_j,b_j), \quad j = 1,2,\ldots,n.\end{aligned} \tag{22}$$

Using the boundary conditions (8) and (9), we obtain

$$\begin{aligned}A_{11}(\alpha) &= B_{11}(\alpha)e^{-2|\alpha|h_1},\\ A_{21}(\alpha) &= B_{21}(\alpha)e^{-2|\alpha|h_1},\\ B_{12}(\alpha) &= A_{12}(\alpha)e^{-2|\alpha|h_2},\\ B_{22}(\alpha) &= A_{22}(\alpha)e^{-2|\alpha|h_2}.\end{aligned} \tag{23}$$

Inserting equations (16) and (17) into equations (20) and (21) and inserting equations (18) and (19) into the boundary conditions (8)–(11), (14), and (15), we obtain

$$\begin{aligned}&c_{44}^{(1)}\left(A_{11}(\alpha)e^{|\alpha|h_1} - B_{11}(\alpha)e^{-|\alpha|h_1}\right)\\ &\quad + e_{15}^{(1)}\left(A_{21}(\alpha)e^{|\alpha|h_1} - B_{21}(\alpha)e^{-|\alpha|h_1}\right) = 0,\end{aligned} \tag{24}$$

$$\begin{aligned}&c_{44}^{(2)}\left(A_{12}(\alpha)e^{-|\alpha|h_2} - B_{12}(\alpha)e^{|\alpha|h_2}\right)\\ &\quad + e_{15}^{(2)}\left(A_{22}(\alpha)e^{-|\alpha|h_2} - B_{22}(\alpha)e^{|\alpha|h_2}\right) = 0,\end{aligned} \tag{25}$$

$$\begin{aligned}&e_{15}^{(1)}\left(A_{11}(\alpha)e^{|\alpha|h_1} - B_{11}(\alpha)e^{-|\alpha|h_1}\right)\\ &\quad + \varepsilon_{11}^{(1)}\left(A_{21}(\alpha)e^{|\alpha|h_1} - B_{21}(\alpha)e^{-|\alpha|h_1}\right) = 0,\end{aligned} \tag{26}$$

$$\begin{aligned}&e_{15}^{(2)}\left(A_{12}(\alpha)e^{-|\alpha|h_2} - B_{12}(\alpha)e^{|\alpha|h_2}\right)\\ &\quad - \varepsilon_{11}^{(2)}\left(A_{22}(\alpha)e^{-|\alpha|h_2} - B_{22}(\alpha)e^{|\alpha|h_2}\right) = 0,\end{aligned} \tag{27}$$

$$\begin{aligned}&c_{44}^{(1)}\left(A_{11}(\alpha) - B_{11}(\alpha)\right) + e_{15}^{(1)}\left(A_{21}(\alpha) - B_{21}(\alpha)\right)\\ &\quad = c_{44}^{(2)}\left(A_{12}(\alpha) - B_{12}(\alpha)\right) + e_{15}^{(2)}\left(A_{22}(\alpha) - B_{22}(\alpha)\right),\end{aligned} \tag{28}$$

$$\begin{aligned}&e_{15}^{(1)}\left(A_{11}(\alpha) - B_{11}(\alpha)\right) - \varepsilon_{11}^{(1)}\left(A_{21}(\alpha) - B_{21}(\alpha)\right)\\ &\quad = e_{15}^{(2)}\left(A_{12}(\alpha) - B_{12}(\alpha)\right) - \varepsilon_{11}^{(2)}\left(A_{22}(\alpha) - B_{22}(\alpha)\right),\end{aligned} \tag{29}$$

$$A_{11}(\alpha)+B_{11}(\alpha)-A_{12}(\alpha)-B_{12}(\alpha) = \frac{i}{\alpha}\int_{a_j}^{b_j} g_W^{(j)}(t)e^{i\alpha t}dt = F_1, \tag{30}$$

$$A_{21}(\alpha)+B_{21}(\alpha)-A_{22}(\alpha)-B_{22}(\alpha) = \frac{i}{\alpha}\int_{a_j}^{b_j} g_\Phi^{(j)}(t)e^{i\alpha t}dt = F_2. \tag{31}$$

Equations (25)–(32) can be written in the form of matrix as follows:

$$\mathbf{A}\cdot\mathbf{B}=\mathbf{C}, \tag{32}$$

where

$$\mathbf{A}=\begin{bmatrix} c_{44}^{(1)}e^{|\alpha|h_1} & -c_{44}^{(1)}e^{|\alpha|h_1} & 0 & 0 & e_{15}^{(1)}e^{|\alpha|h_1} & -e_{15}^{(1)}e^{|\alpha|h_1} & 0 & 0 \\ 0 & 0 & c_{44}^{(2)}e^{-|\alpha|h_2} & -c_{44}^{(2)}e^{-|\alpha|h_2} & 0 & 0 & e_{15}^{(2)}e^{-|\alpha|h_2} & -e_{15}^{(2)}e^{-|\alpha|h_2} \\ e_{15}^{(1)}e^{|\alpha|h_1} & -e_{15}^{(1)}e^{|\alpha|h_1} & 0 & 0 & -\varepsilon_{11}^{(1)}e^{|\alpha|h_1} & \varepsilon_{11}^{(1)}e^{|\alpha|h_1} & 0 & 0 \\ 0 & 0 & e_{15}^{(2)}e^{-|\alpha|h_2} & -e_{15}^{(2)}e^{-|\alpha|h_2} & 0 & 0 & -\varepsilon_{11}^{(2)}e^{-|\alpha|h_2} & \varepsilon_{11}^{(2)}e^{-|\alpha|h_2} \\ c_{44}^{(1)} & -c_{44}^{(1)} & -c_{44}^{(2)} & c_{44}^{(2)} & e_{15}^{(1)} & -e_{15}^{(1)} & -e_{15}^{(2)} & e_{15}^{(2)} \\ e_{15}^{(1)} & -e_{15}^{(1)} & -e_{15}^{(2)} & e_{15}^{(2)} & -\varepsilon_{11}^{(1)} & \varepsilon_{11}^{(1)} & \varepsilon_{11}^{(2)} & -\varepsilon_{11}^{(2)} \\ 1 & 1 & -1 & -1 & 0 & 0 & 0 & 0 \\ 0 & 0 & 0 & 0 & 1 & 1 & -1 & -1 \end{bmatrix}, \tag{33}$$

$$\mathbf{B}=\left[A_{11},B_{11},A_{12},B_{12},A_{21},B_{21},A_{22},B_{22}\right]^T,$$

$$\mathbf{C}=\left[0,0,0,0,0,0,F_1,F_2\right]^T.$$

Solving the linear equation (32), we obtain

$$\begin{aligned} A_{11}(\alpha)&=\frac{H_1F_1+H_2F_2}{H}, \\ A_{12}(\alpha)&=\frac{H_3F_1+H_4F_2}{H}, \\ B_{11}(\alpha)&=\frac{H_5F_1+H_6F_2}{H}, \\ B_{12}(\alpha)&=\frac{H_7F_1+H_8F_2}{H}, \\ A_{21}(\alpha)&=\frac{H_9F_1+H_{10}F_2}{H}, \\ A_{22}(\alpha)&=\frac{H_{11}F_1+H_{12}F_2}{H}, \\ B_{21}(\alpha)&=\frac{H_{13}F_1+H_{14}F_2}{H}, \\ B_{22}(\alpha)&=\frac{H_{15}F_1+H_{16}F_2}{H}. \end{aligned} \tag{34}$$

The expressions of H and H_q, $q=1,2,\ldots,16$, are given in Appendix.

Obviously, the unknown functions $A_{m1}(\alpha)$, $A_{m2}(\alpha)$ and $B_{m1}(\alpha)$, $B_{m2}(\alpha)$ $(m=1,2)$ depend on F_1 and F_2 and, consequently, on the density functions $g_W^{(j)}(x)$ and $g_\Phi{}^{(j)}(x)$. Once F_1 and F_2 are determined, the stress expressions and electric displacement expressions could be obtained.

For this, by substituting equations (16) and (17) into equations (4) and (5), we obtain

$$\begin{aligned} \sigma_{yz}(x,y)=\frac{1}{2\pi}\int_{-\infty}^{+\infty}\Bigg(&\frac{c_{44}^{(2)}|\alpha|e^{|\alpha|y}}{H}\Big[\left(H_3-H_7e^{-2|\alpha|y}\right)F_1 \\ &+\left(H_4-H_8e^{-2|\alpha|y}\right)F_2\Big]+\frac{e_{15}^{(2)}|\alpha|e^{|\alpha|y}}{H} \\ &\cdot\Big[\left(H_{11}-H_{15}e^{-2|\alpha|y}\right)F_1 \\ &+\left(H_{12}-H_{16}e^{-2|\alpha|y}\right)F_2\Big]\Bigg)e^{-i\alpha x}d\alpha, \end{aligned} \tag{35}$$

$$\begin{aligned} D_y(x,y)=\frac{1}{2\pi}\int_{-\infty}^{+\infty}&\frac{e_{15}^{(2)}|\alpha|e^{|\alpha|y}}{H}\Big[\left(H_3-H_7e^{-2|\alpha|y}\right)F_1 \\ &+\left(H_4-H_8e^{-2|\alpha|y}\right)F_2\Big]+\frac{\varepsilon_{11}^{(2)}|\alpha|e^{|\alpha|y}}{H} \\ &\cdot\Big[\left(H_{11}-H_{15}e^{-2|\alpha|y}\right)F_1 \\ &+\left(H_{12}-H_{16}e^{-2|\alpha|y}\right)F_2\Big]e^{-i\alpha x}d\alpha. \end{aligned} \tag{36}$$

Next, we need to transform equations (35) and (36) into singular integral equations of the first kind with Cauchy

kernel. In another form, the integral equations (35) and (36) will be

$$\sigma_{yz}(x,0^-) = \lim_{y\longrightarrow 0^-} \frac{1}{2\pi}\int_{-\infty}^{+\infty}\left(\frac{|\alpha|e^{|\alpha|y}}{H}\left[\left(c_{44}^{(2)}H_3 - c_{44}^{(2)}H_7 + e_{15}^{(2)}H_{11} - e_{15}^{(2)}H_{15}\right)F_1 + \left(c_{44}^{(2)}H_4 - c_{44}^{(2)}H_8 + e_{15}^{(2)}H_{12} - e_{15}^{(2)}H_{16}\right)F_2\right]\right)e^{-i\alpha x}d\alpha = -\sigma_0, \tag{37}$$

$$D_y(x,0^-) = \lim_{y\longrightarrow 0^-} \frac{1}{2\pi}\int_{-\infty}^{+\infty}\left(\frac{|\alpha|e^{|\alpha|y}}{H}\left[\left(e_{15}^{(2)}H_3 - e_{15}^{(2)}H_7 + \varepsilon_{11}^{(2)}H_{11} - \varepsilon_{11}^{(2)}H_{15}\right)F_1 + \left(e_{15}^{(2)}H_4 - e_{15}^{(2)}H_8 + \varepsilon_{11}^{(2)}H_{12} - \varepsilon_{11}^{(2)}H_{16}\right)F_2\right]\right)e^{-i\alpha x}d\alpha = -D_0, \tag{38}$$

where

$$\begin{aligned} Q_1(\alpha) &= c_{44}^{(2)}H_3 - c_{44}^{(2)}H_7 + e_{15}^{(2)}H_{11} - e_{15}^{(2)}H_{15}, \\ Q_2(\alpha) &= c_{44}^{(2)}H_4 - c_{44}^{(2)}H_8 + e_{15}^{(2)}H_{12} - e_{15}^{(2)}H_{16}, \\ Q_3(\alpha) &= e_{15}^{(2)}H_3 - e_{15}^{(2)}H_7 + \varepsilon_{11}^{(2)}H_{11} - \varepsilon_{11}^{(2)}H_{15}, \\ Q_4(\alpha) &= e_{15}^{(2)}H_4 - e_{15}^{(2)}H_8 + \varepsilon_{11}^{(2)}H_{12} - \varepsilon_{11}^{(2)}H_{16}. \end{aligned} \tag{39}$$

Equations (37) and (38) can be rewritten in the following forms:

$$\frac{1}{2\pi}\int_{-\infty}^{+\infty}\frac{|\alpha|e^{|\alpha|y}}{H}Q_1F_1e^{-i\alpha x}d\alpha + \frac{1}{2\pi}\int_{-\infty}^{+\infty}\frac{|\alpha|e^{|\alpha|y}}{H}Q_2F_2e^{-i\alpha x}d\alpha = -\sigma_0, \tag{40}$$

$$\frac{1}{2\pi}\int_{-\infty}^{+\infty}\frac{|\alpha|e^{|\alpha|y}}{H}Q_3F_1e^{-i\alpha x}d\alpha + \frac{1}{2\pi}\int_{-\infty}^{+\infty}\frac{|\alpha|e^{|\alpha|y}}{H}Q_4F_2e^{-i\alpha x}d\alpha = -D_0. \tag{41}$$

By substituting the expressions of F_1 and F_2 into equations (40) and (41), we obtain

$$\begin{aligned} &\frac{1}{2\pi}\int_{-\infty}^{+\infty}\frac{i|\alpha|Q_1e^{|\alpha|y}}{\alpha H}\left(\int_{a_j}^{b_j}g_W^{(j)}(t)e^{i\alpha t}dt\right)e^{-i\alpha x}d\alpha + \frac{1}{2\pi}\int_{-\infty}^{+\infty}\frac{|\alpha|Q_2e^{|\alpha|y}}{\alpha H}\left(\int_{a_j}^{b_j}g_\Phi^{(j)}(t)e^{i\alpha t}dt\right)e^{-i\alpha x}d\alpha = -\sigma_0, \\ &\frac{1}{2\pi}\int_{-\infty}^{+\infty}\frac{i|\alpha|Q_3e^{|\alpha|y}}{\alpha H}\left(\int_{a_j}^{b_j}g_W^{(j)}(t)e^{i\alpha t}dt\right)e^{-i\alpha x}d\alpha + \frac{1}{2\pi}\int_{-\infty}^{+\infty}\frac{|\alpha|Q_4e^{|\alpha|y}}{\alpha H}\left(\int_{a_j}^{b_j}g_\Phi^{(j)}(t)e^{i\alpha t}dt\right)e^{-i\alpha x}d\alpha = -D_0. \end{aligned} \tag{42}$$

Through changing the order of the integration, we obtain

$$\begin{aligned} &\frac{1}{2\pi}\int_{a_j}^{b_j}\left(\int_{-\infty}^{+\infty}\frac{i|\alpha|Q_1e^{|\alpha|y}}{\alpha H}e^{i\alpha(t-x)}d\alpha\right)g_W^{(j)}(t)dt + \frac{1}{2\pi}\int_{a_j}^{b_j}\left(\int_{-\infty}^{+\infty}\frac{|\alpha|Q_2e^{|\alpha|y}}{\alpha H}e^{i\alpha(t-x)}d\alpha\right)g_\Phi^{(j)}(t)dt = -\sigma_0, \\ &\frac{1}{2\pi}\int_{a_j}^{b_j}\left(\int_{-\infty}^{+\infty}\frac{i|\alpha|Q_3e^{|\alpha|y}}{\alpha H}e^{i\alpha(t-x)}d\alpha\right)g_W^{(j)}(t)dt + \frac{1}{2\pi}\int_{a_j}^{b_j}\left(\int_{-\infty}^{+\infty}\frac{|\alpha|Q_4e^{|\alpha|y}}{\alpha H}e^{i\alpha(t-x)}d\alpha\right)g_\Phi^{(j)}(t)dt = -D_0. \end{aligned} \tag{43}$$

On the cracks' surface,

$$\int_{a_j}^{b_j}\left(\frac{Q_{1*}}{H_*}\frac{1}{t-x} + k_1(x,t)\right)g_W^{(j)}(t)dt + \int_{a_j}^{b_j}\left(\frac{Q_{2*}}{H_*}\frac{1}{t-x} + k_2(x,t)\right)g_\Phi^{(j)}(t)dt = -\pi\sigma_0, \tag{45}$$

$$\int_{a_j}^{b_j}\left(\frac{Q_{3*}}{H_*}\frac{1}{t-x} + k_3(x,t)\right)g_W^{(j)}(t)dt + \int_{a_j}^{b_j}\left(\frac{Q_{4*}}{H_*}\frac{1}{t-x} + k_4(x,t)\right)g_\Phi^{(j)}(t)dt = -\pi D_0, \tag{46}$$

where

$$\begin{aligned}
Q_{1*} &= c_{44}^{(1)}c_{44}^{(2)}\left(\varepsilon_{11}^{(1)}-\varepsilon_{11}^{(2)}\right)-\left(e_{15}^{(1)}c_{44}^{(2)}-e_{15}^{(1)}e_{15}^{(2)}\right)\\
&\quad\cdot\left(c_{44}^{(2)}-c_{44}^{(1)}\right)-c_{44}^{(1)}e_{15}^{(2)}\left(e_{15}^{(2)}-e_{15}^{(1)}\right),\\
Q_{2*} &= e_{15}^{(1)}c_{44}^{(2)}\left(\varepsilon_{11}^{(1)}-\varepsilon_{11}^{(2)}\right)+\varepsilon_{11}^{(1)}e_{15}^{(2)}\left(c_{44}^{(2)}-c_{44}^{(1)}\right)\\
&\quad-\left(\varepsilon_{11}^{(1)}c_{44}^{(2)}+e_{15}^{(1)}e_{15}^{(2)}\right)\left(e_{15}^{(2)}-e_{15}^{(1)}\right),\\
Q_{3*} &= c_{44}^{(1)}e_{15}^{(2)}\left(\varepsilon_{11}^{(1)}-\varepsilon_{11}^{(2)}\right)-\left(e_{15}^{(1)}e_{15}^{(2)}-e_{15}^{(1)}e_{15}^{(2)}\right)\\
&\quad\cdot\left(c_{44}^{(2)}-c_{44}^{(1)}\right)-c_{44}^{(1)}\varepsilon_{11}^{(2)}\left(e_{15}^{(2)}-e_{15}^{(1)}\right),\\
Q_{4*} &= e_{15}^{(1)}e_{15}^{(2)}\left(\varepsilon_{11}^{(1)}-\varepsilon_{11}^{(2)}\right)+\varepsilon_{11}^{(1)}\varepsilon_{11}^{(2)}\left(c_{44}^{(2)}-c_{44}^{(1)}\right)\\
&\quad-\left(\varepsilon_{11}^{(1)}e_{15}^{(2)}+e_{15}^{(1)}\varepsilon_{11}^{(2)}\right)\left(e_{15}^{(2)}-e_{15}^{(1)}\right),\\
H_* &= \left(e_{15}^{(2)}-e_{15}^{(1)}\right)^2-\left(c_{44}^{(2)}-c_{44}^{(1)}\right)\left(\varepsilon_{11}^{(1)}-\varepsilon_{11}^{(2)}\right),
\end{aligned} \tag{47}$$

$$\begin{aligned}
k_1(x,t) &= \int_0^\infty\left(\frac{Q_1(\alpha)}{H}-\frac{Q_{1*}}{H_*}\right)\sin(\alpha(t-x))d\alpha,\\
k_2(x,t) &= \int_0^\infty\left(\frac{Q_2(\alpha)}{H}-\frac{Q_{2*}}{H_*}\right)\sin(\alpha(t-x))d\alpha,\\
k_3(x,t) &= \int_0^\infty\left(\frac{Q_3(\alpha)}{H}-\frac{Q_{3*}}{H_*}\right)\sin(\alpha(t-x))d\alpha,\\
k_4(x,t) &= \int_0^\infty\left(\frac{Q_4(\alpha)}{H}-\frac{Q_{4*}}{H_*}\right)\sin(\alpha(t-x))d\alpha.
\end{aligned}$$

Ultimately, equations (4) and (5) are reduced to coupling the first-kind Cauchy singular integral equations.

In equations (45) and (46), $g_W^{(j)}(t)$ and $g_\Phi^{(j)}(t)$ are unknown functions with the following conditions:

$$\begin{aligned}
&\int_{a_j}^{b_j} g_W^{(j)}(t)dt = 0,\\
&\int_{a_j}^{b_j} g_\Phi^{(j)}(t)dt = 0, \quad j = 1,2,\ldots,n.
\end{aligned} \tag{48}$$

By the principle of superposition and mixed boundary conditions, equations (45) and (46) can be formulated as

$$\begin{aligned}
&\sum_{j=1}^{n}\left(\int_{a_j}^{b_j}\left(\frac{Q_{1*}}{H_*}\frac{1}{t_j-x_k}+k_1(x_k,t_j)\right)g_W^{(j)}(t_j)dt_j\right.\\
&\quad\left.+\int_{a_j}^{b_j}\left(\frac{Q_{2*}}{H_*}\frac{1}{t_j-x_k}+k_2(x_k,t_j)\right)g_\Phi^{(j)}(t_j)dt_j\right) = -\pi\sigma_0,\\
&\qquad x_k\in(a_k,b_k),\ j,\ k = 1,2,\ldots,n,
\end{aligned} \tag{49}$$

$$\begin{aligned}
&\sum_{j=1}^{n}\left(\int_{a_j}^{b_j}\left(\frac{Q_{3*}}{H_*}\frac{1}{t_j-x_k}+k_3(x_k,t_j)\right)g_W^{(j)}(t_j)dt_j\right.\\
&\quad\left.+\int_{a_j}^{b_j}\left(\frac{Q_{4*}}{H_*}\frac{1}{t_j-x_k}+k_4(x_k,t_j)\right)g_\Phi^{(j)}(t_j)dt_j\right) = -\pi D_0,\\
&\qquad x_k\in(a_k,b_k),\ j,\ k = 1,2,\ldots,n.
\end{aligned} \tag{50}$$

4. Resolution of Singular Integral Equations

4.1. Normalization of Singular Integral Equations. For the convenience of numerical calculations, we define the normalized quantities as follows:

$$\begin{aligned}
r_j &= \frac{x_j-c_{0j}}{a_{0j}},\\
s_j &= \frac{t_j-c_{0j}}{a_{0j}},
\end{aligned} \tag{51}$$

$$\begin{aligned}
g_W^{(j)}(x) &= f_1^{(j)}(x),\\
g_\Phi^{(j)}(x) &= f_2^{(j)}(x),\\
k_i(x,t) &= L_i(r,s), \quad i = 1,2,3,4,
\end{aligned} \tag{52}$$

$$\begin{aligned}
a_{0j} &= \frac{b_j-a_j}{2},\\
c_{0j} &= \frac{b_j+a_j}{2}, \quad j = 1,2,\ldots,n.
\end{aligned} \tag{53}$$

Using equations (51) and (52), the integral equations (49) and (50) can be expressed as

$$\sum_{j=1}^{n}\left(\int_{-1}^{1}\left(\frac{Q_{1*}}{H_*}\frac{a_{0j}}{a_{0j}s_j+c_{0j}-a_{0k}r_k-c_{0k}}+a_{0j}L_1\left(r_k,s_j\right)\right)\right.$$
$$\cdot f_1^{(j)}\left(s_j\right)ds_j+\int_{-1}^{1}\left(\frac{Q_{2*}}{H_*}\frac{a_{0j}}{a_{0j}s_j+c_{0j}-a_{0k}r_k-c_{0k}}\right.$$
$$\left.\left.+a_{0j}L_2\left(r_k,s_j\right)\right)f_2^{(j)}\left(s_j\right)ds_j\right)=-\pi\sigma_0, \tag{54}$$

$$\sum_{j=1}^{n}\left(\int_{-1}^{1}\left(\frac{Q_{3*}}{H_*}\frac{a_{0j}}{a_{0j}s_j+c_{0j}-a_{0k}r_k-c_{0k}}+a_{0j}L_3\left(r_k,s_j\right)\right)\right.$$
$$\cdot f_1^{(j)}\left(s_j\right)ds_j+\int_{-1}^{1}\left(\frac{Q_{4*}}{H_*}\frac{a_{0j}}{a_{0j}s_j+c_{0j}-a_{0k}r_k-c_{0k}}\right.$$
$$\left.\left.+a_{0j}L_4\left(r_k,s_j\right)\right)f_2^{(j)}\left(s_j\right)ds_j\right)=-\pi D_0. \tag{55}$$

The dislocation density functions $f_1^{(j)}(s_j)$ and $f_2^{(j)}(s_j)$ $(j=1,2,\ldots,n)$ in equations (54) and (55) have the squareroot-type singularity. So we can express $f_1^{(j)}(s_j)=(1/\sqrt{1-s_j^2})\cdot g_1^{(j)}(s_j)\pi\sigma_0$, where $g_1^{(j)}(s_j)$ is a continuous function defined in the interval $[-1,1]$. In the same way, $f_2^{(j)}(s_j)$ may be expressed as

$$f_1^{(j)}\left(s_j\right)=\frac{g_1^{(j)}\left(s_j\right)}{\sqrt{1-s_j^2}}\pi\sigma_0, \tag{56}$$

$$f_2^{(j)}\left(s_j\right)=\frac{g_2^{(j)}\left(s_j\right)}{\sqrt{1-s_j^2}}\pi D_0,\quad j=1,2,\ldots,n. \tag{57}$$

Using the Chebyshev collocation method, one can transform equations (54), (55), and (48) into the system of algebraic equations as follows:

$$\frac{1}{N}\sum_{R=0}^{N}\chi_R\sum_{j=1}^{n}\left[\left(\frac{Q_{1*}}{H_*}\frac{a_{0j}}{a_{0j}s_{jR}+c_{0j}-a_{0k}r_{kq}-c_{0k}}+a_{0j}L_1\left(r_{kq},s_{jR}\right)\right)g_1^{(j)}\left(s_{jR}\right)\right.$$
$$\left.+\left(\frac{Q_{2*}}{H_*}\frac{a_{0j}}{a_{0j}s_{jR}+c_{0j}-a_{0k}r_{kq}-c_{0k}}+a_{0j}L_2\left(r_{kq},s_{jR}\right)\right)g_2^{(j)}\left(s_{jR}\right)\right]=-1, \tag{58}$$

$$\frac{1}{N}\sum_{R=0}^{N}\chi_R\sum_{j=1}^{n}\left[\left(\frac{Q_{3*}}{H_*}\frac{a_{0j}}{a_{0j}s_{jR}+c_{0j}-a_{0k}r_{kq}-c_{0k}}+a_{0j}L_3\left(r_{kq},s_{jR}\right)\right)g_1^{(j)}\left(s_{jR}\right)\right.$$
$$\left.+\left(\frac{Q_{4*}}{H_*}\frac{a_{0j}}{a_{0j}s_{jR}+c_{0j}-a_{0k}r_{kq}-c_{0k}}+a_{0j}L_4\left(r_{kq},s_{jR}\right)\right)g_2^{(j)}\left(s_{jR}\right)\right]=-1, \tag{59}$$

$$\sum_{R=0}^{N}\chi_R g_1^{(k)}\left(s_{kR}\right)=0,$$
$$\sum_{R=0}^{N}\chi_R g_2^{(k)}\left(s_{kR}\right)=0,\quad k=1,2,\ldots,n,\quad q=1,2,\ldots,N, \tag{60}$$

where

$$\chi_0=\chi_N=\frac{1}{2},$$
$$\chi_1=\cdots=\chi_{N-1}=1,$$
$$r_{kq}=\cos\frac{(2q-1)\pi}{2N},$$
$$s_{jR}=\cos\frac{R\pi}{N}. \tag{61}$$

N is the node number of the quadrature formula and s_{jR} and r_{kq} are the zero points of the first and second kinds of Chebyshev polynomials. Equations (58)–(60) are solved numerically to get the solutions of $g_1^{(j)}(s_j)$ and $g_2^{(j)}(s_j)$, which can permit to get the stress and electric displacement.

4.2. Fracture Parameters. The intensity factors are defined by [4]

$$K_\sigma^{a_j}=\lim_{x\longrightarrow a_j^-}\sqrt{2\pi\left(a_j-x\right)}\sigma_{yz}(x,0), \tag{62}$$

$$K_\sigma^{b_j}=\lim_{x\longrightarrow b_j^+}\sqrt{2\pi\left(x-b_j\right)}\sigma_{yz}(x,0), \tag{63}$$

$$K_D^{a_j}=\lim_{x\longrightarrow a_j^-}\sqrt{2\pi\left(a_j-x\right)}D_y(x,0), \tag{64}$$

$$K_D^{b_j} = \lim_{x \longrightarrow b_j^+} \sqrt{2\pi\left(x - b_j\right)} D_y(x,0), \quad j = 1, 2, \ldots, n. \tag{65}$$

According to equations (45) and (46), the singular parts of $\sigma_{yz}(x,0)$ and $D_y(x,0)$ are

$$\begin{aligned}\lim_{x \longrightarrow a_j^-} \sigma_{yz}(x,0) = {} & \frac{Q_{1*}}{H_*} \lim_{s_j \longrightarrow -1^-} \int_{-1}^{1} \frac{f_1^{(j)}\left(s_j\right)}{s_j - x_j} ds_j \\ & + \frac{Q_{2*}}{H_*} \lim_{s_j \longrightarrow -1^-} \int_{-1}^{1} \frac{f_2^{(j)}\left(s_j\right)}{s_j - x_j} ds_j,\end{aligned} \tag{66}$$

$$\begin{aligned}\lim_{x \longrightarrow a_j^-} D_y(x,0) = {} & \frac{Q_{3*}}{H_*} \lim_{s_j \longrightarrow -1^-} \int_{-1}^{1} \frac{f_1^{(j)}\left(s_j\right)}{s_j - x_j} ds_j \\ & + \frac{Q_{4*}}{H_*} \lim_{s_j \longrightarrow -1^-} \int_{-1}^{1} \frac{f_2^{(j)}\left(s_j\right)}{s_j - x_j} ds_j,\end{aligned} \tag{67}$$

$$\begin{aligned}\lim_{x \longrightarrow b_j^+} \sigma_{yz}(x,0) = {} & \frac{Q_{1*}}{H_*} \lim_{s_j \longrightarrow 1^+} \int_{-1}^{1} \frac{f_1^{(j)}\left(s_j\right)}{s_j - x_j} ds_j \\ & + \frac{Q_{2*}}{H_*} \lim_{s_j \longrightarrow 1^+} \int_{-1}^{1} \frac{f_2^{(j)}\left(s_j\right)}{s_j - x_j} ds_j,\end{aligned} \tag{68}$$

$$\begin{aligned}\lim_{x \longrightarrow b_j^+} D_y(x,0) = {} & \frac{Q_{3*}}{H_*} \lim_{s_j \longrightarrow 1^+} \int_{-1}^{1} \frac{f_1^{(j)}\left(s_j\right)}{s_j - x_j} ds_j \\ & + \frac{Q_{4*}}{H_*} \lim_{s_j \longrightarrow 1^+} \int_{-1}^{1} \frac{f_2^{(j)}\left(s_j\right)}{s_j - x_j} ds_j.\end{aligned} \tag{69}$$

Substituting equations (56) and (57) into equations (66)–(69), we obtain

$$\begin{aligned}\lim_{x \longrightarrow a_j^-} \sigma_{yz}(x,0) = {} & \frac{\sigma_0 Q_{1*}}{H_*} \lim_{s_j \longrightarrow -1^-} \frac{g_1^{(j)}(-1)}{\sqrt{s_j^2 - 1}} \\ & + \frac{\sigma_0 Q_{2*}}{H_*} \lim_{s_j \longrightarrow -1^-} \frac{g_2^{(j)}(-1)}{\sqrt{s_j^2 - 1}},\end{aligned} \tag{70}$$

$$\begin{aligned}\lim_{x \longrightarrow b_j^+} \sigma_{yz}(x,0) = {} & \frac{\sigma_0 Q_{1*}}{H_*} \lim_{s_j \longrightarrow 1^+} \frac{-g_1^{(j)}(1)}{\sqrt{s_j^2 - 1}} \\ & + \frac{\sigma_0 Q_{2*}}{H_*} \lim_{s_j \longrightarrow -1^-} \frac{-g_2^{(j)}(1)}{\sqrt{s_j^2 - 1}},\end{aligned} \tag{71}$$

$$\begin{aligned}\lim_{x \longrightarrow a_j^-} D_y(x,0) = {} & \frac{D_0 Q_{3*}}{H_*} \lim_{s_j \longrightarrow -1^-} \frac{g_1^{(j)}(-1)}{\sqrt{s_j^2 - 1}} \\ & + \frac{D_0 Q_{4*}}{H_*} \lim_{s_j \longrightarrow -1^-} \frac{g_2^{(j)}(-1)}{\sqrt{s_j^2 - 1}},\end{aligned} \tag{72}$$

$$\begin{aligned}\lim_{x \longrightarrow b_j^+} D_y(x,0) = {} & \frac{D_0 Q_{3*}}{H_*} \lim_{s_j \longrightarrow 1^+} \frac{-g_1^{(j)}(1)}{\sqrt{s_j^2 - 1}} \\ & + \frac{D_0 Q_{4*}}{H_*} \lim_{s_j \longrightarrow -1^-} \frac{-g_2^{(j)}(1)}{\sqrt{s_j^2 - 1}}.\end{aligned} \tag{73}$$

Substituting equations (70)–(73) into equations (62)–(65), we obtain

$$\begin{aligned}K_\sigma^{a_j} &= \sigma_0 \sqrt{\pi a_{0j}} \left[\frac{Q_{1*}}{H_*} g_1^{(j)}(-1) + \frac{Q_{2*}}{H_*} g_2^{(j)}(-1)\right], \\ K_\sigma^{b_j} &= -\sigma_0 \sqrt{\pi a_{0j}} \left[\frac{Q_{1*}}{H_*} g_1^{(j)}(1) + \frac{Q_{2*}}{H_*} g_2^{(j)}(1)\right], \\ K_D^{a_j} &= D_0 \sqrt{\pi a_{0j}} \left[\frac{Q_{3*}}{H_*} g_1^{(j)}(-1) + \frac{Q_{4*}}{H_*} g_2^{(j)}(-1)\right], \\ K_D^{b_j} &= -D_0 \sqrt{\pi a_{0j}} \left[\frac{Q_{3*}}{H_*} g_1^{(j)}(1) + \frac{Q_{4*}}{H_*} g_2^{(j)}(1)\right], \quad j = 1, 2, \ldots, n.\end{aligned} \tag{74}$$

The energy release rate of piezoelectric materials has the following form [24]:

$$G = \frac{1}{4}\left[\omega_1 K_\sigma^2 + \omega_2 K_\sigma K_D + \omega_3 K_D^2\right], \tag{75}$$

where

$$\begin{aligned}\mathbf{K} &= \left[K_\sigma, K_D\right], \\ \omega_1 &= \frac{Q_{4*}}{H_* \mathbf{\Lambda}}, \\ \omega_2 &= \frac{Q_{3*} - Q_{1*}}{H_* \mathbf{\Lambda}}, \\ \omega_3 &= \frac{-Q_{1*}}{H_* \mathbf{\Lambda}}, \\ \mathbf{\Lambda} &= \begin{bmatrix} \frac{Q_{1*}}{H_*} & \frac{Q_{2*}}{H_*} \\ \frac{Q_{3*}}{H_*} & \frac{Q_{4*}}{H_*} \end{bmatrix}.\end{aligned} \tag{76}$$

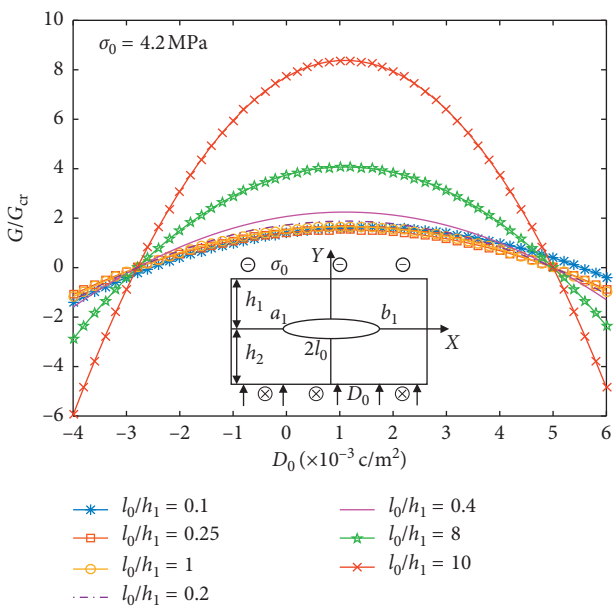

Figure 2: Effects of electric displacement D_0 on the energy release rate for different l_0/h_1.

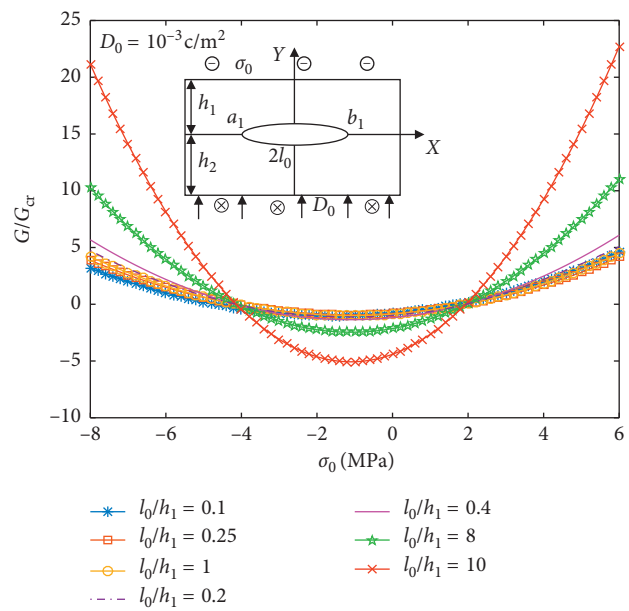

Figure 3: Effects of stress σ_0 on the energy release rate for different l_0/h_1.

5. Numerical Process and Results

This section is divided into two parts. Firstly, some numerical applications to verify the obtained solutions are given, in the case when we have a single interface crack. Then, the influence of material constants on the energy release rate is studied when we have multiple interface cracks.

Initially, we assume that the piezoelectric substrate is the PZT-5H ceramic. Its parameters are given as [2]

$$\begin{aligned} c_{44}^{(2)} &= 3.53 \times 10^{10}\ \mathrm{N/m^2}, \\ e_{15}^{(2)} &= 17.0\ \mathrm{C/m^2}, \\ \varepsilon_{11}^{(2)} &= 1.51 \times 10^{-8}\ \mathrm{C/Vm}, \\ G_{cr} &= 5\ \mathrm{N/m}, \end{aligned} \tag{77}$$

where superscript 2 represents the substrate material.

5.1. A Single Interface Crack. To validate the solution, we chose the case that material 1 is a fine-grained coating made of PZT-5H ceramics by plasma spraying technology and material 2 is normal PZT-5H ceramics (where 1 and 2 represent the fine-grained coating and substrate material, respectively), which means that material 1 and material 2 have approximately the same piezoelectric and dielectric constants under suitable conditions, and the elastic modulus of material 1 is larger than that of material 2. So $c_{44}^{(1)}/c_{44}^{(2)} = 2.5$, $h_1/h_2 = 1/100$, and the single interface crack of $l_0 = 5$ mm loaded by an antiplane stress of $\sigma_0 = 4.2$ MPa and a variable electric displacement D_0 are considered. The curves of the energy release rate G/G_{cr} as a function of D_0 under different values of l_0/h_1 are plotted (Figure 2). Then, the same interface crack is loaded by an electric displacement D_0 of 10^{-3} c/m^2 and a variable stress σ_0. For different values of l_0/h_1, the curves G/G_{cr} as a function of σ_0 are plotted (Figure 3).

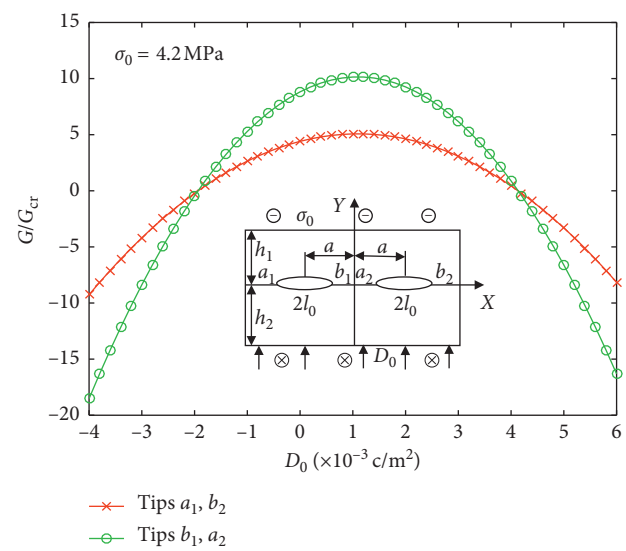

Figure 4: Effects of stress σ_0 on the energy release rate for double identical interface cracks.

5.1.1. Studies of the Effect of Stress σ_0 and Electric Displacement D_0 on Energy Release Rate. Effects of electric displacement D_0 and stress σ_0 on the energy release rate for different l_0/h_1 are shown in Figures 2 and 3, respectively.

5.2. Multiple Interface Cracks. The interaction between multiple interface cracks is investigated. The distance between double interface crack centers is chosen as $a/l_0 = a/l_1 = 6/5$ (where $l_0 = l_1 = 5$ mm, $l_2 = 3$ mm, and $h_1 = 5$ mm

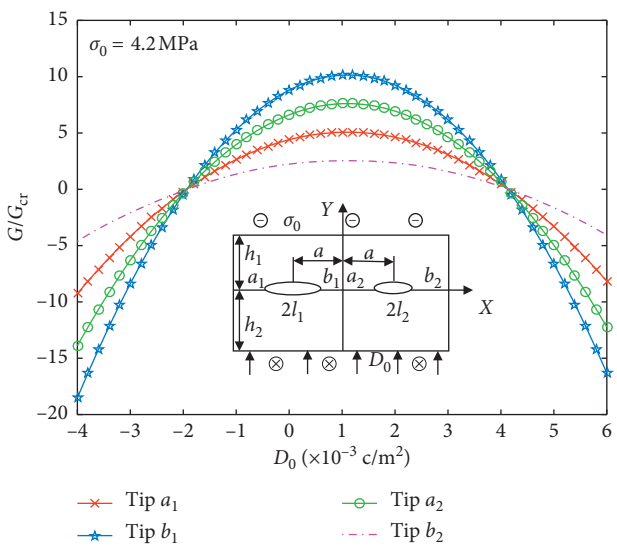

Figure 5: Effects of stress σ_0 on the energy release rate for double different interface cracks.

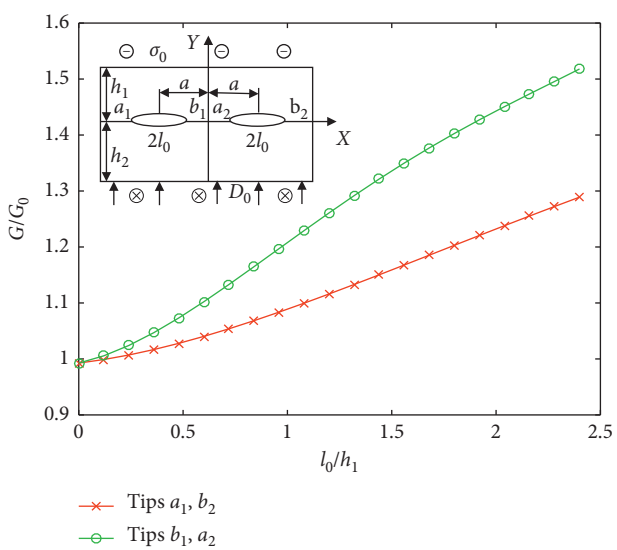

Figure 6: Effects of l_0/h_1 on the energy release rate for double identical interface cracks.

and other material parameters are the same as in the previous selection). The influences of electric displacement D_0 on the normalized energy release rate G/G_{cr} are shown in Figures 4 and 5 and the change rules of the normalized energy release rate G/G_0 and the value of l/h_1 are shown in Figures 6–8 for the interaction between three identical and different Griffith cracks. The rules of the normalized energy release rate G/G_0 versus the value of l/h_1 are shown in Figures 9 and 10 (where $a/l_0 = a/l_1 = 6/5$, $l_0 = l_1 = 5$ mm, $l_2 = 3$ mm, $l_3 = 2.5$ mm, $h_1 = 5$ mm, and $G_0 = \lim_{l/h_1 \longrightarrow 0} G$ and other material parameters are the same as in the previous selection).

5.2.1. Studies of the Effect of Stress σ_0 and Electric Displacement D_0 on Energy Release Rate for Double Griffith Interface Cracks. Effects of electric displacement D_0 and stress σ_0 on the energy release rate for double Griffith interface cracks are shown in Figures 4 and 5.

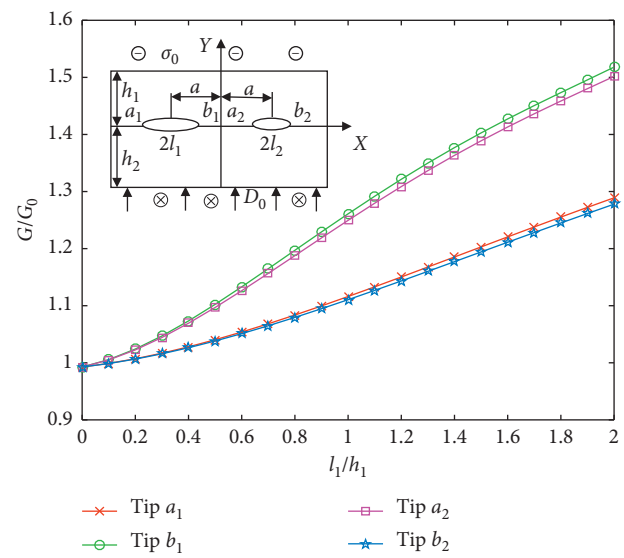

Figure 7: Effects of l_1/h_1 on the energy release rate for double different interface cracks.

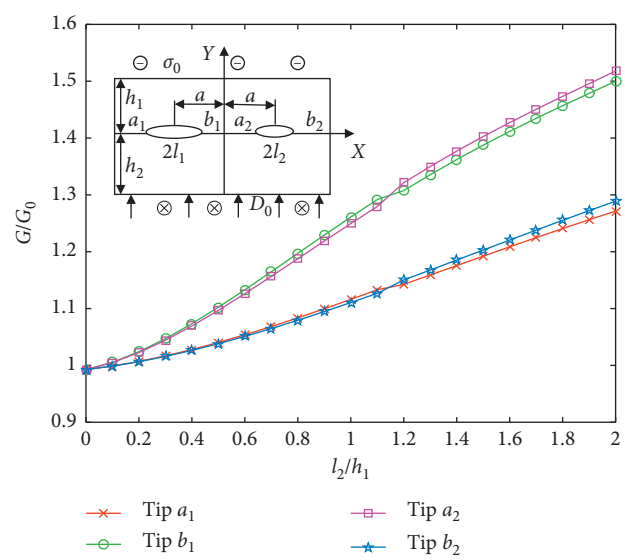

Figure 8: Effects of l_1/h_1 on the energy release rate for double different interface cracks.

5.2.2. Studies of the Influence of l/h_1 on Energy Release Rate for Double Interface Cracks. Effects of l/h_1 on the energy release rate for double Griffith interface cracks are shown in Figures 6–8.

5.2.3. Studies of the Influence of l/h_1 on Energy Release Rate for Three Interface Cracks. Effects of l/h_1 on the energy release rate for three interface cracks are shown in Figures 9 and 10.

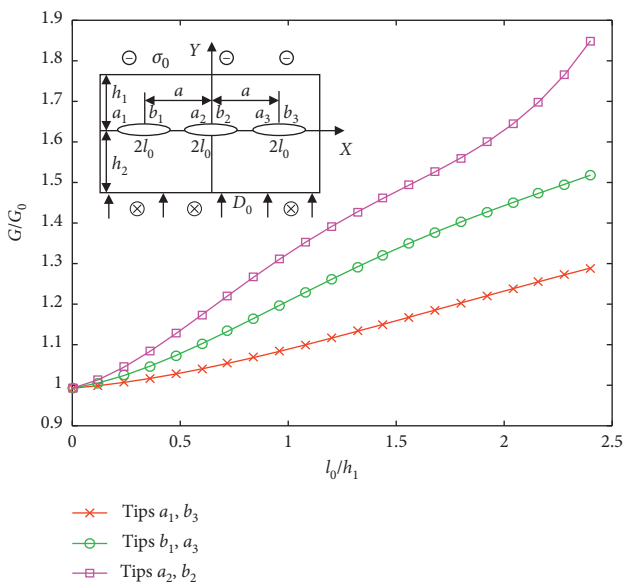

Figure 9: Effects of l_1/h_1 on the energy release rate for three identical interface cracks.

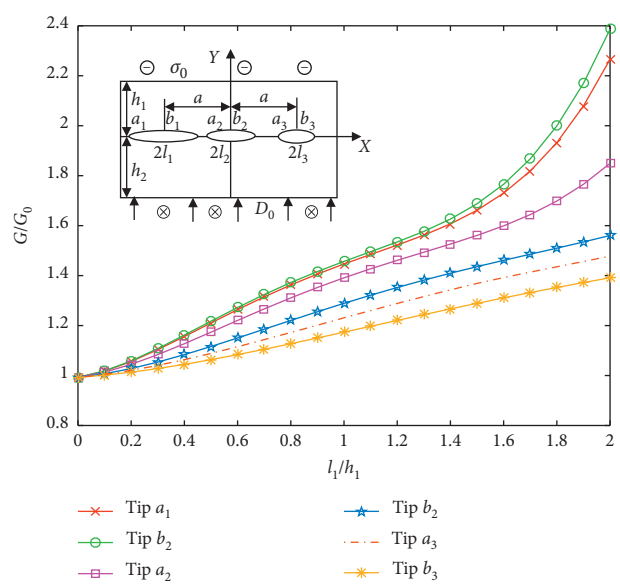

Figure 10: Effects of l_1/h_1 on the energy release rate for three different interface cracks.

6. Results and Discussion

Figure 2 displays the variation of the normalized energy release rate G/G_{cr} against the applied electric displacement D_0. It can be clearly seen that by varying l_0/h_1, the curves G/G_{cr} are parabolas, and as D_0 decreases from zero, G/G_{cr} always decreases. However, when D_0 increases from zero, G/G_{cr} firstly increases and then begins to decrease. The results show that negative electric displacement loading always prevents crack propagation and positive electric displacement loading may prompt or prevent crack propagation, which are consistent with the conclusions of Pak et al. [4, 10, 13]. However, the peak energy release rate of the fine-grained piezoelectric coating/substrate structure is higher than that of the large-grained piezoelectric coating/substrate structure.

Figure 3 indicates the effects of applied stress σ_0 on the normalized energy release rate G/G_{cr}. It can be easily seen that as stress σ_0 increases from zero, G/G_{cr} always increases. When the stress σ_0 decreases from zero, the G/G_{cr} first decreases and then increases, and it indicates the initial closure of a crack followed by a type of crack propagation due to compressive loading. The results indicate that stress loading may prompt or retard crack propagation.

The diversification of the normalized energy release rate G/G_{cr} versus the applied electric displacement D_0 for double identical and different interface cracks is shown in Figures 4 and 5. It is found that the variation of the energy release rate against the applied electric displacement is similar to that shown in Figure 2. However, the normalized energy release rate of the double interface crack has a larger peak compared to that shown in Figure 2. Moreover, the peak values of the energy release rate near the crack tips b_1, a_2 are larger than those near the crack tips a_1, b_2. Because of symmetry when the length of double interface cracks is equal, the variations of the energy release rate near the crack tips b_1, a_2 and a_1, b_2 are the same.

Figures 6–8 present the effects of the values of l/h_1 (where l stands for the crack length) on the normalized energy release rate G/G_0 for double identical and different interface cracks. We found that the energy release rate increased with the increase of l/h_1. The change rate of the inner crack tips is higher with the variation of l/h_1 than that of the outer crack tips. The lines in Figure 8 intersect with the variation of l/h_1 in this case; if the double cracks have the same length, they are consistent with previous conclusions.

Figures 9 and 10 illustrate the change rule of the normalized energy release rate G/G_0 and l/h_1 for three identical and different interface cracks. The results reflect that the values of the energy release rate susceptible to l/h_1 near the inner crack tips are larger than those that approach the outer crack tips, regardless of the number of cracks. At the same time, we noticed that when the value of thickness of coating h_1 was small, the value of the energy release rate was large, which indicated that the structure was more safe when the coating was thin. This reflects the superiority of the fine-grained piezoelectric material structure because it can make the structure thinner.

7. Conclusions

In this paper, multiple Griffith cracks at the interface of a fine-grained piezoelectric coating/substrate are studied. The variation of the energy release rate with applied stress, electric displacement, crack length, and coating thickness is demonstrated. Based on the change rule of the energy release rate and various parameters, the following conclusions are drawn:

(1) The interaction between cracks, applied electromechanical loads, and coating thickness has a great influence on the energy release rate for Griffith interface cracks. Moreover, the negative electric

displacement loading always prevents crack propagation, and positive electric displacement loading may prompt or delay crack propagation. Furthermore, the appropriate stress loading can restrain the crack growth. Therefore, in the practical application of engineering, we can choose the appropriate load to ensure the safety of the structure.

(2) For a bimaterial structure, compared with previous works [10, 13], we found that the peak of the energy release rate at the crack tips of a fine-grained piezoelectric coating/substrate interface is larger than that at the crack tips of a large-grained piezoelectric material/substrate structure interface, and thus, the fine-grained piezoelectric coating/substrate structure has safer material properties. Therefore, in order to better resist fractures, fine-grained piezoelectric materials are a better choice in engineering.

Nomenclature

a_j, b_j:	Left and right tips of arbitrary interface cracks
$A_{1k}(\alpha)$:	Unknown functions satisfying the loading displacement $W(x, y)$
$A_{2k}(\alpha)$:	Unknown functions satisfying the electric field $\Phi(x, y)$
$\mathbf{A}$:	The coefficient matrix of linear equations with unknown functions $A_{1k}(\alpha)$, $B_{1k}(\alpha)$, $A_{2k}(\alpha)$, and $B_{2k}(\alpha)$
$B_{1k}(\alpha)$:	Unknown functions satisfying the loading displacement $W(x, y)$
$B_{2k}(\alpha)$:	Unknown functions satisfying the electric field $\Phi(x, y)$
$\mathbf{B}$:	Unknown functions $A_{1k}(\alpha)$, $B_{1k}(\alpha)$, $A_{2k}(\alpha)$, and $B_{2k}(\alpha)$
$c_{44}^{(k)}$:	Elastic modulus
$\mathbf{C}$:	The constant terms of linear equations with unknown functions $A_{1k}(\alpha)$, $B_{1k}(\alpha)$, $A_{2k}(\alpha)$, and $B_{2k}(\alpha)$
D_0:	Electric displacement
D_x and D_y:	Electric displacement components
F_1:	Integral expression with unknown functions $g_W^{(j)}(x)$
F_2:	Integral expression with unknown functions $g_\Phi^{(j)}(x)$
$g_1^{(j)}(s_j)$ and $g_2^{(j)}(s_j)$:	Continuous functions defined in the interval $[-1, 1]$
$g_W^{(j)}(x)$:	Unknown functions with the condition $\int_{a_j}^{b_j} g_W^{(j)}(t)dt = 0$
$g_\Phi^{(j)}(x)$:	Unknown functions with the condition $\int_{a_j}^{b_j} g_\Phi^{(j)}(t)dt = 0$
G_{cr}:	Critical crack extension force
G:	Energy release rate
h_1:	Thickness of the coating
h_2:	Thickness of the substrate
H_*:	Limit value of H when α tends to infinity
H_q:	Combination of $e^{-2\lvert\alpha\rvert h_1}$, $e^{-2\lvert\alpha\rvert h_2}$, and $e^{-4\lvert\alpha\rvert h_1}$
H:	Combination of $e^{-2\lvert\alpha\rvert h_1}$ and $e^{-2\lvert\alpha\rvert h_2}$
$K_\sigma^{a_j}$:	Stress intensity factor at the left tip of the arbitrary interface crack
$K_\sigma^{b_j}$:	Stress intensity factor at the right tip of the arbitrary interface crack
$K_D^{a_j}$:	Electric displacement intensity factor at the left tip of the arbitrary interface crack
$K_D^{b_j}$:	Electric displacement intensity factor at the right tip of the arbitrary interface crack
$\mathbf{K}$:	Intensity factors
l:	Crack length
N:	The node number of the quadrature formula
Q_{i^*}:	Limit value of Q_i when α tends to infinity
Q_i:	Linear combination of H_q
r_{kq}:	Zero points of the second kind of Chebyshev polynomials
s_{jR}:	Zero points of the first kind of Chebyshev polynomials
U and V:	In-plane displacement
W:	Out-of-plane displacement
X:	X-axis of the rectangular space coordinate system
Y:	Y-axis of the rectangular space coordinate system
Z:	Z-axis of the rectangular space coordinate system
σ_0:	Stress
σ_{xz} and σ_{yz}:	Stress components
$e_{15}^{(k)}$:	Piezoelectric constants
$\varepsilon_{11}^{(k)}$:	Dielectric constants
Φ:	In-plane electric fields
∇^2:	Two-dimensional Laplacian operator
$\mathbf{\Lambda}$:	Matrix composed of Q_{i^*} and H_*.

Appendix

The expressions of H and H_q, $q = 1, 2, \ldots, 16$, are as follows:

$$
\begin{aligned}
a_1 &= \left(1-e^{-2|\alpha|h_2}\right)\left(1+e^{-2|\alpha|h_1}\right)c_{44}^{(2)} - \left(1-e^{-2|\alpha|h_1}\right)\left(1+e^{-2|\alpha|h_2}\right)c_{44}^{(1)},\\
a_2 &= \left(1-e^{-2|\alpha|h_2}\right)\left(1+e^{-2|\alpha|h_1}\right)e_{15}^{(2)} - \left(1-e^{-2|\alpha|h_1}\right)\left(1+e^{-2|\alpha|h_2}\right)e_{15}^{(1)},\\
a_3 &= -\left(1-e^{-2|\alpha|h_2}\right)\left(1+e^{-2|\alpha|h_1}\right)\varepsilon_{11}^{(2)} + \left(1-e^{-2|\alpha|h_1}\right)\left(1+e^{-2|\alpha|h_2}\right)\varepsilon_{11}^{(1)},\\
H &= a_2^2 - a_1 a_3,\\
H_1 &= \frac{e^{-2|\alpha|h_1}\left(a_2^2 - a_1 a_3\right) + e^{-2|\alpha|h_1}\left(1+e^{-2|\alpha|h_1}\right)\left(1-e^{-4|\alpha|h_1}\right)\left(c_{44}^{(1)}a_3 - e_{15}^{(1)}a_2\right)}{\left(1+e^{-2|\alpha|h_1}\right)},\\
H_2 &= \frac{e^{-2|\alpha|h_1}\left(1+e^{-2|\alpha|h_1}\right)\left(1-e^{-4|\alpha|h_1}\right)\left(e_{15}^{(1)}a_3 - \varepsilon_{11}^{(1)}a_2\right)}{\left(1+e^{-2|\alpha|h_1}\right)},\\
H_3 &= \left(1-e^{-4|\alpha|h_1}\right)\left(c_{44}^{(1)}a_3 - e_{15}^{(1)}a_2\right),\\
H_4 &= \left(1-e^{-4|\alpha|h_1}\right)\left(e_{15}^{(1)}a_3 - \varepsilon_{11}^{(1)}a_2\right),\\
H_5 &= \frac{a_2^2 - a_1 a_3 + \left(1+e^{-2|\alpha|h_1}\right)\left(1-e^{-4|\alpha|h_1}\right)\left(c_{44}^{(1)}a_3 - e_{15}^{(1)}a_2\right)}{\left(1+e^{-2|\alpha|h_1}\right)},\\
H_6 &= \frac{\left(1+e^{-2|\alpha|h_1}\right)\left(1-e^{-4|\alpha|h_1}\right)\left(e_{15}^{(1)}a_3 - \varepsilon_{11}^{(1)}a_2\right)}{\left(1+e^{-2|\alpha|h_1}\right)},\\
H_7 &= e^{-2|\alpha|h_2}\left(1-e^{-4|\alpha|h_1}\right)\left(c_{44}^{(1)}a_3 - e_{15}^{(1)}a_2\right),\\
H_8 &= e^{-2|\alpha|h_2}\left(1-e^{-4|\alpha|h_1}\right)\left(e_{15}^{(1)}a_3 - \varepsilon_{11}^{(1)}a_2\right),\\
H_9 &= \frac{e^{-2|\alpha|h_1}\left(a_2^2 - a_1 a_3\right) + e^{-2|\alpha|h_1}\left(1+e^{-2|\alpha|h_1}\right)\left(1-e^{-4|\alpha|h_1}\right)\left(e_{15}^{(1)}a_1 - c_{44}^{(1)}a_2\right)}{\left(1+e^{-2|\alpha|h_1}\right)},\\
H_{10} &= \frac{e^{-2|\alpha|h_1}\left(1+e^{-2|\alpha|h_1}\right)\left(1-e^{-4|\alpha|h_1}\right)\left(\varepsilon_{11}^{(1)}a_1 - e_{15}^{(1)}a_2\right)}{\left(1+e^{-2|\alpha|h_1}\right)},\\
H_{11} &= \left(1-e^{-4|\alpha|h_1}\right)\left(e_{15}^{(1)}a_1 - c_{44}^{(1)}a_2\right),\\
H_{12} &= \left(1-e^{-4|\alpha|h_1}\right)\left(\varepsilon_{11}^{(1)}a_1 - e_{15}^{(1)}a_2\right),\\
H_{13} &= \frac{a_2^2 - a_1 a_3 + \left(1+e^{-2|\alpha|h_1}\right)\left(1-e^{-4|\alpha|h_1}\right)\left(e_{15}^{(1)}a_1 - c_{44}^{(1)}a_2\right)}{\left(1+e^{-2|\alpha|h_1}\right)},\\
H_{14} &= \frac{\left(1+e^{-2|\alpha|h_1}\right)\left(1-e^{-4|\alpha|h_1}\right)\left(\varepsilon_{11}^{(1)}a_1 - e_{15}^{(1)}a_2\right)}{\left(1+e^{-2|\alpha|h_1}\right)},\\
H_{15} &= e^{-2|\alpha|h_2}\left(1-e^{-4|\alpha|h_1}\right)\left(e_{15}^{(1)}a_1 - c_{44}^{(1)}a_2\right),\\
H_{16} &= e^{-2|\alpha|h_2}\left(1-e^{-4|\alpha|h_1}\right)\left(\varepsilon_{11}^{(1)}a_1 - e_{15}^{(1)}a_2\right).
\end{aligned}
\tag{A.1}
$$

Data Availability

All the numerical calculation data used to support the findings of this study can be obtained by calculating the equations in this paper, and piezoelectric material parameters are taken from reference [1]. The codes used in this paper are available from the corresponding author upon request.

Conflicts of Interest

The authors declare that there are no conflicts of interest regarding the publication of this paper.

Acknowledgments

This study was funded by the National Natural Science Foundation of China (51775361).

References

[1] V. Govorukha, M. Kamlah, V. Loboda, and Y. Lapusta, "Interface cracks in piezoelectric materials," *Smart Materials and Structures*, vol. 25, no. 2, pp. 023001–023021, 2016.

[2] S. B. Park and C. T. Sun, "Fracture criteria for piezoelectric ceramics," *Journal of the American Ceramic Society*, vol. 78, no. 6, pp. 1475–1480, 1995.

[3] W. Deng and S. A. Meguid, "Analysis of conducting rigid inclusion at the interface of two dissimilar piezoelectric materials," *Journal of Applied Mechanics*, vol. 65, no. 1, pp. 76–84, 1998.

[4] Y. E. Pak, "Crack extension force in a piezoelectric material," *Journal of Applied Mechanics*, vol. 57, no. 3, pp. 647–653, 1990.

[5] Z. Suo, C.-M. Kuo, D. M. Barnett, and J. R. Willis, "Fracture mechanics for piezoelectric ceramics," *Journal of the Mechanics and Physics of Solids*, vol. 40, no. 4, pp. 739–765, 1992.

[6] T.-Y. Zhang and P. Tong, "Fracture mechanics for a mode III crack in a piezoelectric material," *International Journal of Solids and Structures*, vol. 33, no. 3, pp. 343–359, 1996.

[7] V. B. Govorukha and V. V. Loboda, "Contact zone models for an interface crack in a piezoelectric material," *Acta Mechanica*, vol. 140, no. 3-4, pp. 233–246, 2000.

[8] O. Viun, A. Komarov, Y. Lapusta, and V. Loboda, "A polling direction influence on fracture parameters of a limited permeable interface crack in a piezoelectric bi-material," *Engineering Fracture Mechanics*, vol. 191, pp. 143–152, 2018.

[9] M. Li, Y. L. Tian, P. H. Wen, and M. H. Aliabadi, "Anti-plane interfacial crack with functionally graded coating: static and dynamic," *Theoretical and Applied Fracture Mechanics*, vol. 86, pp. 250–259, 2016.

[10] A. K. Soh, D. N. Fang, and K. L. Lee, "Analysis of a bi-piezoelectric ceramic layer with an interfacial crack subjected to anti-plane shear and in-plane electric loading," *European Journal of Mechanics—A/Solids*, vol. 19, no. 6, pp. 961–977, 2000.

[11] N. N. Shavlakadze, "Contact problem of electroelasticity for a piecewise homogeneous piezoelectric plate with an elastic coating," *Journal of Applied Mathematics and Mechanics*, vol. 81, no. 3, pp. 228–235, 2017.

[12] J. W. Shin and T.-U. Kim, "Transient response of a mode III interface crack between piezoelectric layer and functionally graded orthotropic layer," *International Journal of Solids and Structures*, vol. 90, pp. 122–128, 2016.

[13] M. Gherrous and H. Ferdjani, "Analysis of a Griffith crack at the interface of two piezoelectric materials under anti-plane loading," *Continuum Mechanics and Thermodynamics*, vol. 28, no. 6, pp. 1683–1704, 2016.

[14] H. Nan and B. Wang, "Influence of residual surface stress on the fracture of nanoscale piezoelectric materials with conducting cracks," *Science China Physics, Mechanics and Astronomy*, vol. 57, no. 2, pp. 280–285, 2014.

[15] M. Nourazar and M. Ayatollahi, "Analysis of an orthotropic strip containing multiple defects bonded between two piezoelectric layers," *Acta Mechanica*, vol. 227, no. 5, pp. 1293–1306, 2016.

[16] W. Y. Tian and R. K. N. D. Rajapakse, "Fracture parameters of a penny-shaped crack at the interface of a piezoelectric bi-material system," *International Journal of Fracture*, vol. 141, no. 1-2, pp. 37–48, 2006.

[17] C.-F. Gao, H. Kessler, and H. Balke, "Crack problems in magnetoelectroelastic solids. Part II: general solution of collinear cracks," *International Journal of Engineering Science*, vol. 41, no. 9, pp. 983–994, 2003.

[18] S. Kozinov, V. Loboda, and Y. Lapusta, "Periodic set of limited electrically permeable interface cracks with contact zones," *Mechanics Research Communications*, vol. 48, pp. 32–41, 2013.

[19] S. Kim, G. S. Lee, T. R. Shrout, and S. Venkataramani, "Fabrication of fine-grain piezoelectric ceramics using reactive calcination," *Journal of Materials Science*, vol. 26, no. 16, pp. 4411–4415, 1991.

[20] S. D. Yui, H. W. Manabu, and F. H. Shinobu, "Grain size effect on electrical properties of Mn-modified $0.67BiFeO_3$–$0.33BaTiO_3$ lead-free piezoelectric ceramics," *Ceramics International*, vol. 42, no. 7, pp. 8206–8211, 2016.

[21] H. A. Yu, X. H. Wang, J. Fang, and T. Long, "Grain size effect on piezoelectric and ferroelectric properties of $BaTiO_3$ ceramics," *Journal of the European Ceramic Society*, vol. 34, pp. 1445–1448, 2014.

[22] F. Q. Guo, B. H. Zhang, Z. X. Fan et al., "Grain size effects on piezoelectric properties of $BaTiO_3$ ceramics prepared by spark plasma sintering," *Journal of Materials Science: Materials in Electronics*, vol. 27, no. 6, pp. 5967–5971, 2016.

[23] P. Zheng, J. L. Zhang, Y. Q. Tan, and C. L. Wang, "Grain-size effects on dielectric and piezoelectric properties of poled $BaTiO_3$ ceramics," *Acta Materialia*, vol. 60, no. 13-14, pp. 5022–5030, 2012.

[24] B.-L. Wang and Y.-W. Mai, "Multiple surface cracks in a piezoelectric layer bonded to an elastic substrate under transient electromechanical loads," *Mechanics of Materials*, vol. 39, no. 6, pp. 564–579, 2007.